



HHS Public Access

Author manuscript

Bioorg Med Chem Lett. Author manuscript; available in PMC 2018 July 01.

Published in final edited form as:

Bioorg Med Chem Lett. 2017 July 01; 27(13): 2990–2995. doi:10.1016/j.bmcl.2017.05.014.

Challenges in the development of an M₄ PAM preclinical candidate: The discovery, SAR, and *in vivo* characterization of a series of 3-aminoazetidine-derived amides

James C. Tarr^a, Michael R. Wood^{a,c}, Meredith J. Noetzel^{a,b}, Jeanette Bertron^a, Rebecca L. Weiner^{a,a}, Alice L. Rodriguez^a, Atin Lamsal^a, Frank W. Byers^{a,b}, Sichen Chang^{a,b}, Hyekyung P. Cho^a, Carrie K. Jones^{a,b,e}, Colleen M. Niswender^{a,b,e}, Michael W. Wood^d, Nicholas J. Brandon^d, Mark E. Duggan^d, P. Jeffrey Conn^{a,b,e}, Thomas M. Bridges^{a,b,*}, and Craig W. Lindsley^{a,b,c,*}

^aVanderbilt Center for Neuroscience Drug Discovery, Vanderbilt University School of Medicine, Nashville, TN 37232, USA

^bDepartment of Pharmacology, Vanderbilt University School of Medicine, Nashville, TN 37232, USA

^cDepartment of Chemistry, Vanderbilt University, Nashville, TN 37232, USA

^dNeuroscience Innovative Medicines, Astra Zeneca, 141 Portland Street, Cambridge, MA 02139, USA

^eVanderbilt Kennedy Center, Vanderbilt University School of Medicine, Nashville, TN 37232, USA

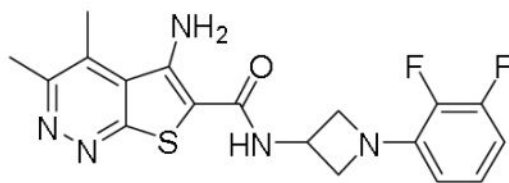
Abstract

This letter details the continued chemical optimization of a novel series of M₄ positive allosteric modulators (PAMs) based on a 5-amino-thieno[2,3-*c*]pyridazine core by incorporating a 3-amino azetidine amide moiety. The analogs described within this work represent the most potent M₄ PAMs reported for this series to date. The SAR to address potency, clearance, subtype selectivity, CNS exposure, and P-gp efflux are described. This work culminated in the discovery of VU6000918, which demonstrated robust efficacy in a rat amphetamine-induced hyperlocomotion reversal model at a minimum efficacious dose of 0.3 mg/kg. 2009 Elsevier Ltd. All rights reserved.

Graphical Abstract

*To whom correspondence should be addressed: thomas.m.bridges@vanderbilt.edu and craig.lindsley@vanderbilt.edu.

Publisher's Disclaimer: This is a PDF file of an unedited manuscript that has been accepted for publication. As a service to our customers we are providing this early version of the manuscript. The manuscript will undergo copyediting, typesetting, and review of the resulting proof before it is published in its final citable form. Please note that during the production process errors may be discovered which could affect the content, and all legal disclaimers that apply to the journal pertain.



17j (VU6000918)

hM₄ EC₅₀ = 19 nM

% ACh_{Max} = 88

rat AHL reversal = 74% (3 mg/kg PO)

Keywords

M₄; Muscarinic acetylcholine receptor; Positive allosteric modulator (PAM); Schizophrenia; Azetidine

Positive allosteric modulators (PAMs) of the muscarinic acetylcholine receptor (M₄) (**1-4**) have emerged as an exciting potential strategy for the treatment of numerous CNS disorders, including schizophrenia,¹⁻²⁰ Huntington's disease,²¹ and Alzheimer's disease.²² Previous reports from our laboratory have described the discovery and characterization of VU0152100 (ML108, **1**), an *in vivo* tool compound which demonstrated efficacy in rodent models of anti-psychotic efficacy.^{3,4} We subsequently reported related congener VU0467154 (**2**), based on a 5-amino-thieno[2,3-*c*]pyridazine core, which, despite its robust *in vivo* activity in multiple preclinical rodent models and a favorable pharmacokinetic (PK) profile, suffered from considerably lower potency at the human M₄ receptor as compared to rat.^{11,19} In the course of our medicinal chemistry campaign to identify a compound with improved potency at the human M₄ receptor while maintaining suitable DMPK properties for a clinical candidate, we encountered steep SAR not only in potency at M₄, but in multiple DMPK properties as well.^{13,14,19,20} Herein, we describe our efforts to replace the benzylic linker present in compounds **1-4** with substituted 3-amino azetidines.

Observing that small cyclic amides afforded potent analogs in both Eli Lilly's and our M₄ PAM programs, we wished to examine the introduction of a cyclic linker between the 5-aminothieno[2,3-*c*]pyridazine amide core and the appended aryl ring. Such a change may serve to decrease the planarity of the molecule, thus reducing its ability to form pi-stacking interactions and thereby improve solubility, restrict the conformations available for the aryl ring to adopt, and remove the benzylic methylene as a potential metabolic soft spot. Diamine linkers would provide a convenient synthetic handle by which to introduce substituents on the cyclic linker. Several potential linkers were examined, including monocyclic and bicyclic diamines; however, 3-amino substituted azetidines yielded the most potent analogs (Figure 2).

Analogs were readily prepared following functionalization of commercially available 3-(Boc-amino)-azetidine via nucleophilic substitution or Buchwald-Hartwig^{23,24} cross-

coupling reactions, followed by Boc deprotection and amide coupling to the thieno[2,3-*c*]pyridazine core (Scheme 1). Our initial library examined the effect of tertiary carbamates, sulfonamides, and amides (Table 1). Basic tertiary azetidine amines were poorly tolerated and led to a sharp decrease in human M₄ (hM₄) potency (data not shown). Carbamates proved to be the most potent compounds in this class, with analog **6b** displaying an EC₅₀ of 23 nM. However, upon further profiling, **6b** was found to have weak activity at human M₂ (hM₂, EC₅₀ = 2.65 μM) and a short elimination half-life *in vivo* in rat (*t*_{1/2} < 30 min) due to facile hydrolysis of the carbamate, which proved to be the case in general for the carbamate series and thus precluded their advancement. Azetidine sulfonamides (**6e**), ureas (**6d**), and amides (**6f-h**) were also tolerated, albeit with lower potency as compared to the carbamates. Compound **6h** was selected for further assessment, which gratifyingly found an improved profile compared to the carbamate series with reduced activity at hM₂ (EC₅₀ > 10 μM) and low *in vivo* clearance (rat CL_p = 3.1 mL/min/kg). Unfortunately, **6h** was found to have low CNS exposure (rat brain:plasma K_p = 0.03, K_{p,uu} = 0.37 at 0.25 hr post-IV cassette dose) likely due to P-gp efflux (MDCK-MDR1 ER = 96).

Encouraged by our initial results within this series, we sought to further improve the azetidine amides by examining *N*-aryl azetidines. Initial efforts sought to mimic the carbamate functionality by incorporating 1,3-heteroaryl substituents (**16a-c**). Compound **16c** maintained reasonable hM₄ potency (EC₅₀ = 106 nM), exhibited moderate *in vitro* clearance (predicted rat and human CL_{hep} = 41 and 12 mL/min/kg, respectively, based on hepatic microsomal CL_{int}), and achieved moderate CNS exposure (rat brain:plasma K_p = 0.17, K_{p,uu} = 1.3). Despite lacking mAChR subtype selectivity (hM₂ EC₅₀ = 220 nM), **16c** was advanced to a rat amphetamine hyperlocomotion (AHL) reversal study where it exhibited marginal efficacy (16% reversal following 10 mg/kg PO) but provided initial proof-of-concept for the azetidine amide class of compounds. Broadening our scope of *N*-heteroaryl azetidines led us to identify numerous potent analogs (**16d-q**). A wide variety of heterocycles was tolerated, with pyridyl, pyrimidyl, and pyrazinyl substituents providing EC₅₀s < 100 nM. Substitution of the heteroaryl ring proved capable of imparting dramatic shifts in potency. While the parent 4-pyridyl azetidine analog possessed micromolar PAM activity (data not shown), introduction of halogen substituents on the 4-pyridyl ring provided exquisitely potent analogs (**16p**, **16q**). Substitution at the *meta*-position was also tolerated on 3-pyridyl analogs, with methoxy (**16l**) and fluorine (**16m**) providing analogs of comparable potency to **16e**.

While we were able to achieve excellent *in vitro* potencies within this series, obtaining both reasonable CNS exposure and metabolic stability proved more challenging. A number of compounds (**16e-h**, **16l**) failed to achieve acceptable CNS exposure (rat brain:plasma K_p < 0.05) and/or were found to be substrates for human P-gp efflux (**16e**, **16i**, **16q**). Additionally, rat *in vivo* PK studies revealed evidence for extrahepatic non-CYP₄₅₀ metabolism in certain cases (**16o**, **16p**; possibly due to aldehyde oxidase-mediated metabolism *alpha* to the 4-pyridyl nitrogen). Increasing the lipophilicity of analogs by incorporation of halogen atoms generally led to modest increases in rat CNS exposure and reduced P-gp efflux. Compound **16j** was selected for further DMPK profiling, which revealed low predicted clearance (human and rat predicted CL_{hep} = 5.6 and 18 mL/min/kg,

respectively, based on hepatic microsomal CL_{int}) and low potential for CYP₄₅₀ inhibition (3A4, 2D6, 2C9, 1A2 $IC_{50} > 30 \mu M$). In a rat (male, Sprague-Dawley; $n = 2$) *in vivo* PK study, **16j** demonstrated low clearance ($CL_p = 8.8 \text{ mL/min/kg}$) with a small volume of distribution ($V_{ss} = 0.89 \text{ L/kg}$) and moderate elimination half-life ($t_{1/2} = 1.3 \text{ hr}$). Total and unbound distribution of **16j** to the brain was moderate in rat (brain:plasma $K_p = 0.12$, $K_{p,uu} = 0.33$ at 0.25 hr post-IV cassette dose), and, while it was still a substrate for human P-gp (ER = 8.5 in MDCK-MDR1 cells), its efflux was attenuated compared to related analogs. Given this favorable profile, it was advanced to a dose-response amphetamine hyperlocomotion (AHL) study in rat where it demonstrated robust reversal of AHL (Figure 3). An oral dose of 1 mg/kg provided a 44% reversal of AHL, and a maximal effect of 55% AHL reversal was achieved from 10 and 30 mg/kg dose levels. This level of *in vivo* efficacy was encouraging for the series and comparable to that previously reported for benchmark compounds **3** and **4**. However, due to **16j**'s P-gp liability and potentiation of hM₂ ($EC_{50} = 0.96 \mu M$, $ACh_{Max} = 43\%$), it was deemed not suitable for further development.

Expanding on the scope of azetidine analogs we had already investigated, we synthesized a library of *N*-aryl analogs (Table 3). Phenyl congener **17a** retained the excellent hM₄ potency that could be attained with *N*-heteroaryl analogs. While **17a** did suffer from higher *in vivo* clearance (rat $CL_p = 45 \text{ mL/min/kg}$), a consequence of phenyl hydroxylation based on *in vitro* metabolic soft-spot experiments (data not shown), as well as moderately potent potentiation of hM₂ ($EC_{50} = 1.78 \mu M$, 58% ACh_{Max}), it showed a promising divergence from the *N*-heteroaryl azetidine SAR with improved CNS exposure (rat brain:plasma $K_p = 0.57$, $K_{p,uu} = 0.73$). Fluorine substitution(s) on the phenyl ring (**17b**, **17h-j**) generally maintained good hM₄ potency and reduced *in vivo* clearance (**17i**, **17j**; rat $CL_p = 4.4$ and 16 mL/min/kg, respectively). Notably, the azetidine congeners (**17f**, **17g**) of benzylic-linked M₄ PAMs previously reported by our group^{19,20} exhibited significantly weaker hM₄ activity compared to that of **17j** (~10-fold and 40-fold, respectively). In light of its favorable potency and rat PK, compound **17j**, bearing a 2,3-difluorophenyl substituent, was selected for additional characterization. Operational model parameters were determined for **17j** from ACh CRC fold-shift experiments (Ca^{2+} mobilization assays), which revealed a rat M₄ K_B of 120 nM and $\alpha\beta$ of 63, a cynomolgus monkey M₄ K_B of 890 nM and $\alpha\beta$ of 120, and a human M₄ K_B of 2000 nM and $\alpha\beta$ of 380. Gratifyingly, **17j** displayed broadly attractive properties including an absence of P-gp efflux (MDCK-MDR1 ER = 1.3), acceptable selectivity versus hM₂ (~230-fold based on potency), and high brain distribution (rat brain:plasma $K_p = 0.77$, $K_{p,uu} = 0.86$ at 0.25 hr post-IV cassette dose).

Based on these findings, compound **17j** was then evaluated in a rat AHL dose response study (Figure 4) where it demonstrated statistically significant AHL reversal (18%) from a low oral dose of 0.03 mg/kg and reached maximal reversal (74%) from a 3 mg/kg dose, with a resulting *in vivo* plasma EC_{50} of 74 nM (0.66 nM unbound) based on terminal concentrations measured in the study animals (1.5 hr post-administration of **17j**).

Compound **17j** was further studied to evaluate its suitability for progression into IND-enabling studies. An Ames test found no evidence of mutagenesis, a large secondary pharmacology panel (Cerep) revealed a fairly clean profile (all $IC_{50}s/EC_{50}s > 25\text{--}30 \mu M$ except for human DAT binding $IC_{50} = 0.45 \mu M$), and CYP₄₅₀ inhibition was acceptable

(1A2 IC₅₀ = 25 μM, 3A4 IC₅₀ = 11 μM, 2D6 IC₅₀ = 14 μM, 2C9 IC₅₀ = 3.8 μM, 2C19 IC₅₀ = 6.3 μM; with no evidence for time-dependent inhibition). IV and PO PK studies with **17j** in rat (male, Sprague Dawley, *n* = 1–3) and dog (female, mongrel, *n* = 1–2) found the compound to possess low to moderate *in vivo* clearance (rat and dog CL_p = 16 and 17 mL/min/kg, respectively) with a small to moderate volume of distribution (rat and dog V_{ss} = 0.67 and 1.6 L/kg, respectively), and moderate oral bioavailability (rat and dog F = 38% and 20%, respectively, from a 2–3 mg/kg solution dose). However, lower oral bioavailability in dog was observed (11%) from a suspension dose (2 mg/kg) in a low-exipient vehicle. These findings, coupled with a low kinetic solubility (solubility in FaSSIF at pH 6.5 after 1 hr = 0.015 mg/mL; aqueous solubility at pH 7.4 = 1.8 μM), as well as suboptimal predicted human PK (~1–2 hr t_{1/2} based on moderate and small predicted CL and V_{ss}, respectively) led us to deprioritize **17j** for further evaluation as a preclinical candidate and focus efforts on overcoming the evident solubility-limited absorption.

In summary, substitution of the benzyl linker with a 3-aminoazetidone moiety afforded facile entry into an extremely potent series of M₄ PAMs. By varying the substitution pattern of *N*-aryl and *N*-heteroaryl groups, we were able to optimize subtype selectivity, clearance, CNS exposure, and P-gp efflux. Compound **17j** demonstrated robust AHL reversal in a rodent model; however, an unacceptably short projected human half-life and low oral bioavailability (due in part to solubility-limited absorption) precluded its advancement as a clinical candidate. Further study and optimization within this series is ongoing, and will be reported in due course.

Acknowledgments

The authors would like to thank NIH (U01MH087965, Vanderbilt, NCDDG). We also thank William K. Warren, Jr. and the William K. Warren Foundation who funded the William K. Warren, Jr. Chair in Medicine (to C.W.L.)

References and notes

1. Chan WY, McKinize DL, Bose S, Mitchell SN, Witkins JM, Thompson RC, Christopoulos A, Birdsall NJ, Bymaster FP, Felder CC. *Proc Natl Acad Sci USA*. 2008; 105:10978–10983. [PubMed: 18678919]
2. Leach K, Loiancono RE, Felder CC, McKinize DL, Mogg A, Shaw DB, Sexton PM, Christopoulos A. *Neuropsychopharmacology*. 2010; 35:855–869. [PubMed: 19940843]
3. Brady A, Jones CK, Bridges TM, Kennedy PJ, Thompson AD, Breininger ML, Gentry PR, Yin H, Jadhav SB, Shirey J, Conn PJ, Lindsley CW. *J Pharm & Exp Ther*. 2008; 327:941–953.
4. Byun NE, Grannan M, Bubser M, Barry RL, Thompson A, Rosanelli J, Gowrishnakar R, Kelm ND, Damon S, Bridges TM, Melancon BJ, Tarr JC, Brogan JT, Avison MJ, Deutch AY, Wess J, Wood MR, Lindsley CW, Gore JC, Conn PJ, Jones CK. *Neuropsychopharmacology*. 2014; 39:1578–1593. [PubMed: 24442096]
5. Farrell M, Roth BL. *Neuropsychopharmacology*. 2010; 35:851–852. [PubMed: 20145632]
6. Jones CK, Byun N, Bubser M. *Neuropsychopharmacology*. 2012; 37:16–42. [PubMed: 21956443]
7. Shirey JK, Xiang Z, Orton D, Brady AE, Johnson KA, Williams R, Ayala JE, Rodriguez AL, Wess J, Weaver D, Niswender CM, Conn PJ. *Nat Chem Bio*. 2008; 4:42–50. [PubMed: 18059262]
8. Le U, Melancon BJ, Bridges TM, Utley TJ, Lamsal A, Vinson PN, Sheffler DJ, Jones CK, Morrison R, Wood MR, Daniels JS, Conn PJ, Niswender CM, Lindsley CW, Hopkins CR. *Bioorg Med Chem Lett*. 2013; 23:346–350. [PubMed: 23177787]
9. Kennedy JP, Bridges TM, Gentry PR, Brogan JT, Brady AE, Shirey JK, Jones CK, Conn PJ, Lindsley CW. *ChemMedChem*. 2009; 4:1600–1607. [PubMed: 19705385]

10. Salovich JM, Sheffler DJ, Vinson PN, Lamsal A, Utley TJ, Blobaum AL, Bridges TM, Le U, Jones CK, Wood MR, Daniels JS, Conn PJ, Niswender CM, Lindsley CW, Hopkins CR. *Bioorg Med Chem Lett.* 2012; 22:5084–5088. [PubMed: 22738637]
11. Bubser M, Bridges TM, Thorbeck DD, Gould RW, Grannan M, Noetzel MJ, Niswender CM, Daniels JS, Melancon BJ, Tarr JC, Wess J, Duggan ME, Brandon NJ, Dunlop J, Wood MW, Wood MR, Lindsley CW, Conn PJ, Jones CK. *ACS Chem Neurosci.* 2014; 5:920–942. [PubMed: 25137629]
12. Smith E, Chase P, Niswender CM, Conn PJ, Lindsley CW, Madoux F, Acosta M, Scampavia L, Spicer T, Hodder P. *J Biomol Screening.* 2015; 20:858–868.
13. Wood MR, Noetzel MJ, Tarr JC, Rodriguez AL, Lamsal A, Chang S, Foster JJ, Smith E, Hodder PS, Engers DW, Niswender CM, Brandon NJ, Wood MW, Duggan ME, Conn PJ, Bridges TM, Lindsley CW. *Bioorg Med Chem Lett.* 2016; 26:4282–4286. [PubMed: 27476142]
14. Wood MR, Noetzel MJ, Engers JL, Bollinger KA, Melancon BJ, Tarr JC, Han C, West M, Gregro AR, Lamsal A, Chang S, Ajmera S, Smith E, Chase P, Hodder PS, Bubser M, Jones CK, Hopkins CR, Emmitte KA, Niswender CM, Wood MW, Duggan ME, Conn PJ, Bridges TM, Lindsley CW. *Bioorg Med Chem Lett.* 2016; 26:3029–3033. [PubMed: 27185330]
15. Szabo M, Huynh T, Valant C, Lane JR, Sexton PM, Christopoulos A, Capuano B. *MedChemComm.* 2015; 6:1998–2003.
16. Huynh T, Valant C, Crosby IT, Sexton PM, Christopoulos A, Capuano B. *ACS Chem Neurosci.* 2015; 6:1592–1599.
17. Croy CH, Schober DA, Xiao H, Quets A, Christopoulos A, Felder CC. *Mol Pharmacol.* 2014; 86:106–115. [PubMed: 24807965]
18. Huynh T, Valant C, Crosby IT, Sexton PM, Christopoulos A, Capuano B. *J Med Chem.* 2013; 56:1592–1599.
19. Wood MR, Noetzel MJ, Poslusey MS, Melancon BJ, Tarr JC, Lamsal A, Chang S, Luscombe VB, Weiner RL, Cho HP, Bubser M, Jones CK, Niswender CM, Wood MW, Engers DW, Brandon NJ, Duggan ME, Conn PJ, Bridges TM, Lindsley CW. *Bioorg Med Chem Lett.* 2017; 27:171–175.
20. a) Wood MR, Noetzel J, Melancon BJ, Poslusney MS, Nance KD, Hurtade MA, Luscombe VB, Weiner RL, Rodriguez AL, Lamsal A, Chang S, Bubser M, Blobaum AL, Engers DW, Niswender CM, Jones CK, Brandon NJ, Wood MW, Duggan ME, Conn PJ, Bridges TM, Lindsley CW. *ACS Med Chem Lett.* 2017; 8:233–238. [PubMed: 28197318] b) Melancon BJ, Wood MR, Noetzel J, Nance KD, Engelberg EM, Han C, Lamsal A, Chang S, Bubser M, Blobaum AL, Engers DW, Niswender CM, Jones CK, Brandon NJ, Wood MW, Duggan ME, Conn PJ, Bridges TM, Lindsley CW. *Bioorg Med Chem Lett.* submitted.
21. Pancani T, Foster DJ, Bichell T, Bradley E, Bridges TM, Klar R, Daniels JS, Jones CK, Bowman AB, Lindsley CW, Xiang Z, Conn PJ. *Proc Natl Acad Sci USA.* 2015; 112:14078–14083. [PubMed: 26508634]
22. Shen W, Plotkin JL, Francardo V, Ko WKD, Xie Z, Li Q, Fieblinger T, Wess J, Neubig RR, Lindsley CW, Conn PJ, Greengrad P, Bezar E, Cenci MA, Surmeier DJ. *Neuron.* 2015; 88:762–773. [PubMed: 26590347]
23. Wolfe JP, Wagaws S, Marcoux JF, Buchwald SL. *Acc Chem Res.* 1998; 31:805.
24. Hartwig JF. *Acc Chem Res.* 1998; 31:852.

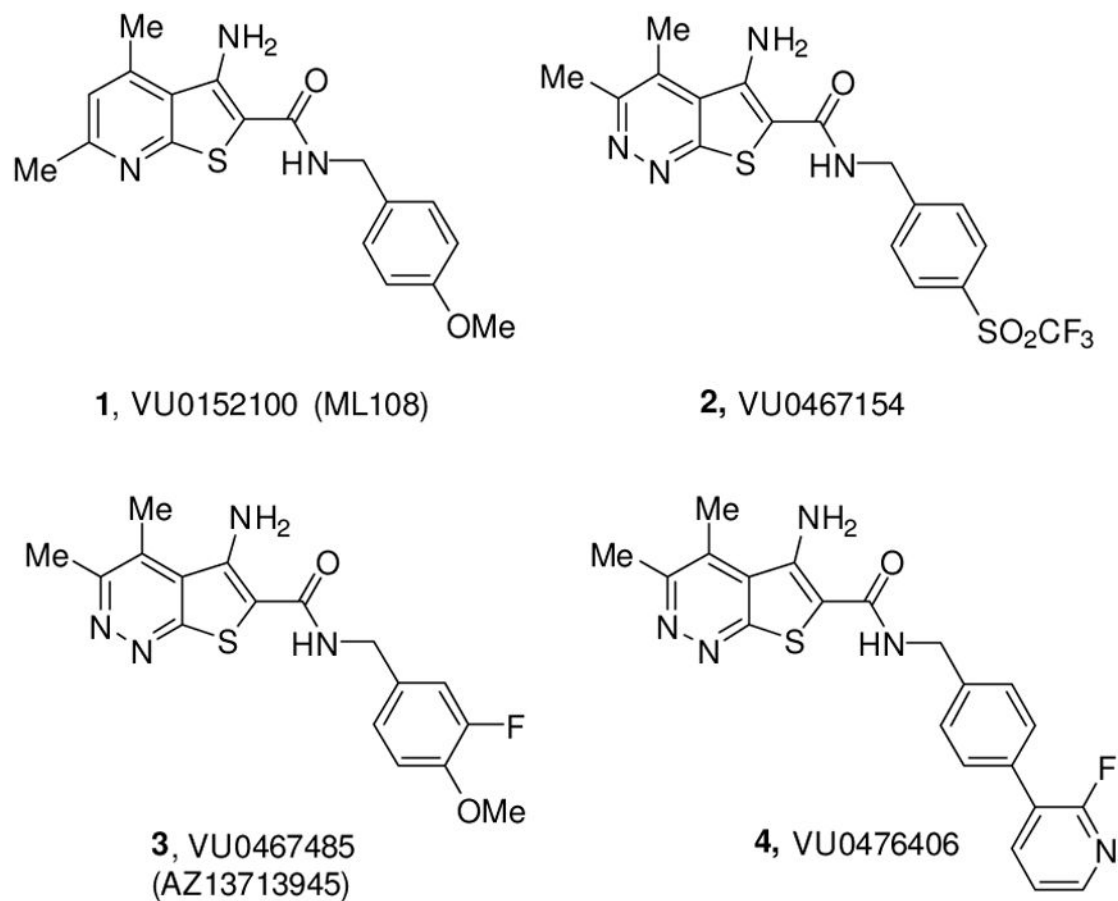


Figure 1. Structures of representative M₄ PAMs **1-4**, highlighting the optimized rodent *in vivo* tool M₄ PAM, VU0467154 (**2**), the clinical candidate VU0467485/AZ13713945 (**3**) and the non-human primate *in vivo* tool VU0476406 (**4**).

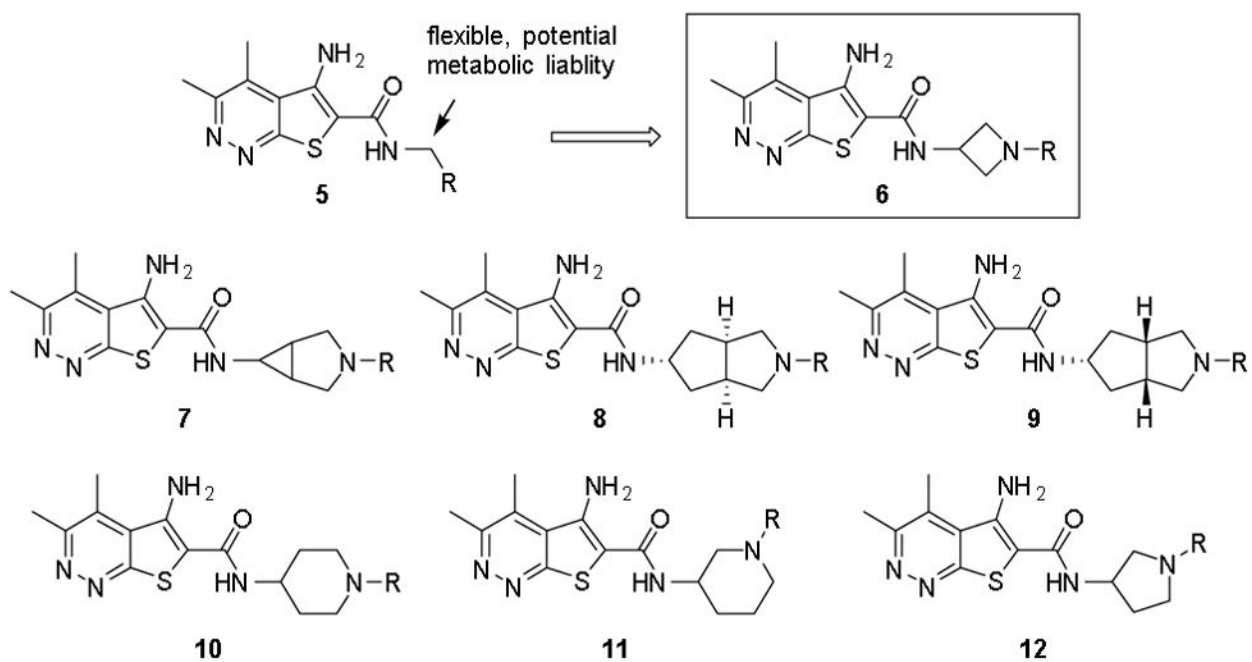


Figure 2.
Cyclic diamines examined as alternative amide linkers to thieno[2,3-*c*]pyridazine core.

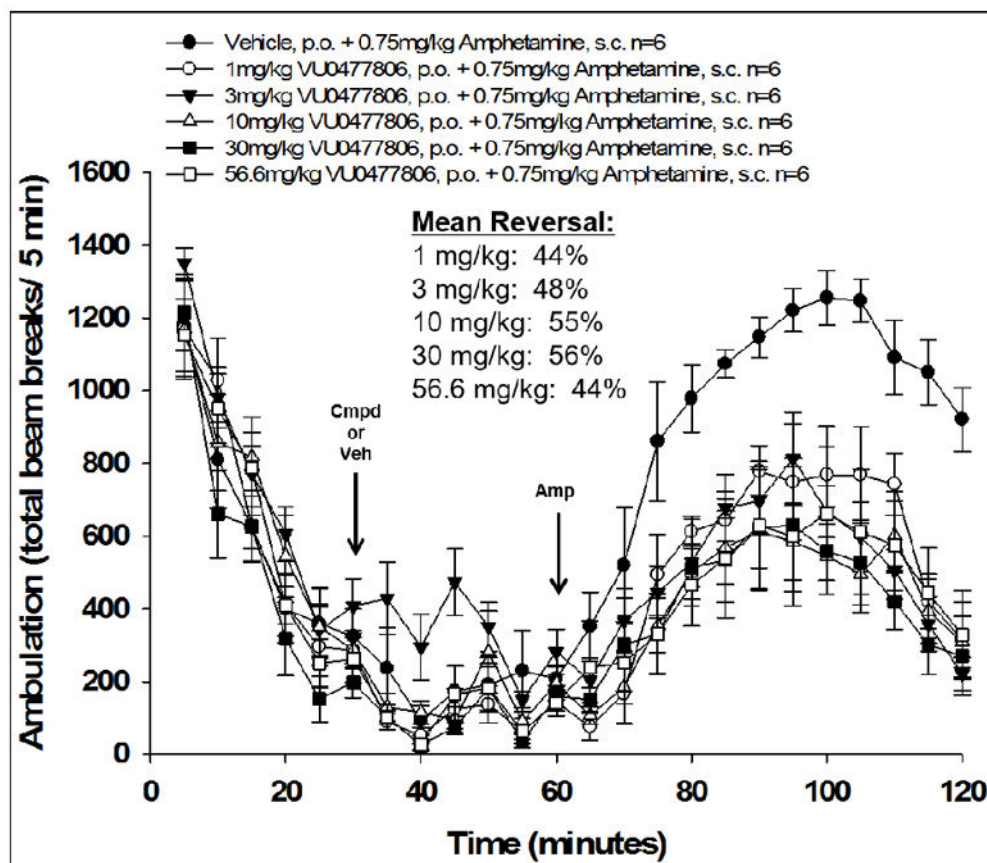


Figure 3.

Reversal of amphetamine-induced hyperlocomotion in rat (male, Sprague Dawley, $n = 6$ per dose group) by **16j** (VU0477806). M_4 PAM or vehicle (10% tween-80 90% water [v/v]) was administered orally 30 min after habituation in the chamber, and then 0.75 mg/kg amphetamine was administered subcutaneously 30 min later ($t = 60$ min). Total ambulations were measured over the subsequent 1 hr interval ($t = 60$ –120 min) and used to calculate %reversal of AHL for each dose group. Data represent means \pm SEM.

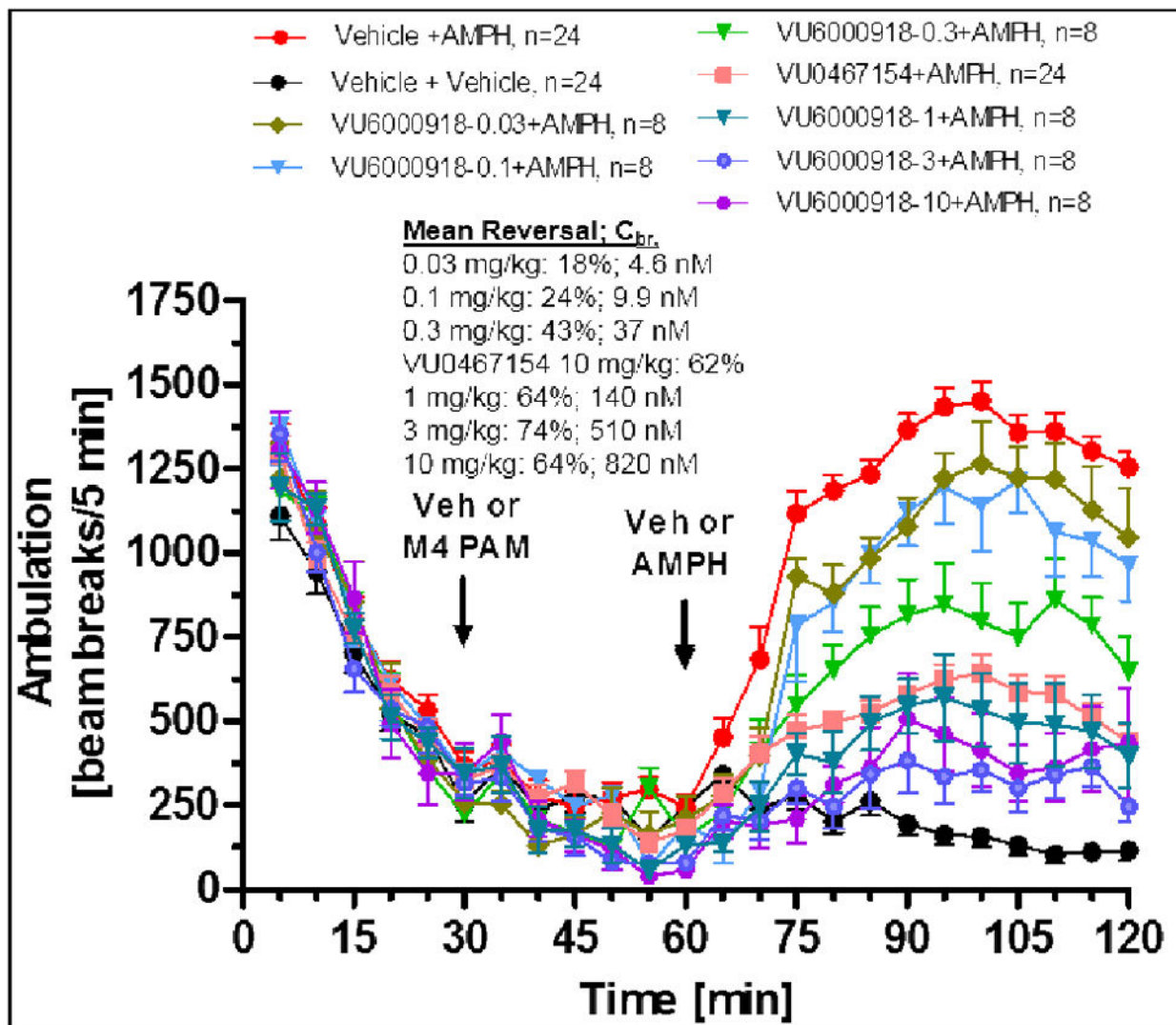
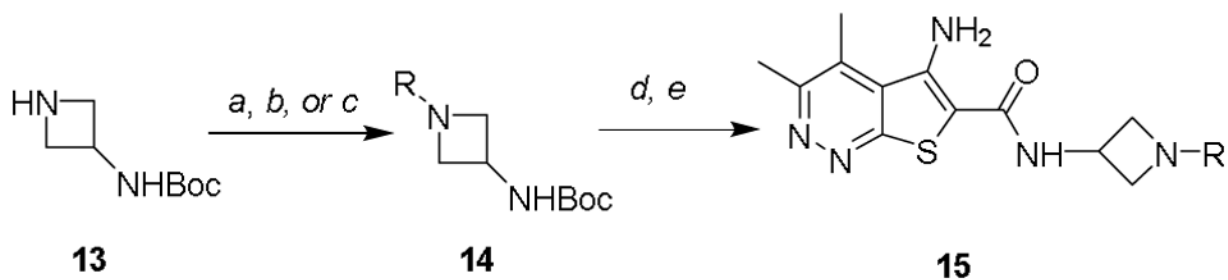
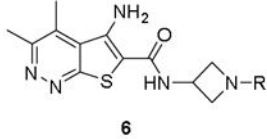


Figure 4. Reversal of amphetamine-induced hyperlocomotion in rat (male, Sprague Dawley, $n = 8-24$ per dose group) by **17j** (VU6000918). M₄ PAM, control M₄ PAM (VU0467154) or vehicle (10% tween-80 90% water [v/v]) was administered orally 30 min after habituation in the chamber, and then 0.75 mg/kg amphetamine or vehicle (100% water) was administered subcutaneously 30 min later ($t = 60$ min). Total ambulations were measured over the subsequent 1 hr interval ($t = 60-120$ min) and used to calculate % reversal of AHL for each dose group. Data represent means \pm SEM.

**Scheme 1.**

Synthesis of M₄ PAM analogs **6**, **16**, **17**. Reagents and conditions: (a) R-X, DCM, DIPEA, rt. (b) R-Het-X, Cs₂CO₃, DMF, heat (c) Ar-X, Pd₂(dba)₃, *rac*-BINAP, Cs₂CO₃, toluene, 100 °C (d) TFA, DCM, rt, 3 hr (e) 5-amino-3,4-dimethylthieno[2,3-*c*]pyridazine-6-carboxylic acid, HATU, DIPEA, DMF, 2 hr.

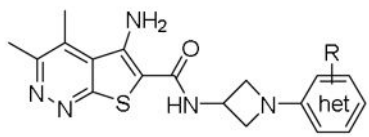
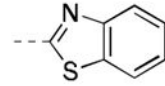
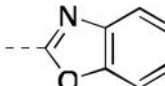
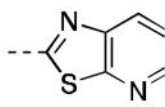
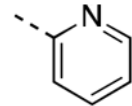
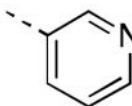
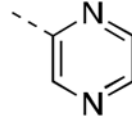
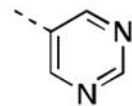
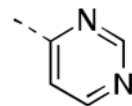
Table 1Structures and activities for M₄ PAM analogs **6**.


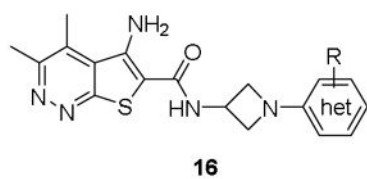
Cmpd	R	hM ₄ EC ₅₀ (nM) ^a [% ACh Max ±SEM]	hM ₄ pEC ₅₀ (±SEM)
6a	CO ₂ Bn	30 [81±8]	7.62±0.19
6b	CO ₂ Ph	23 [96±3]	7.65±0.03
6c	CO ₂ (3-Me)Ph	67 [85±9]	7.23±0.17
6d	C(O)NHPH	217 [89±6]	6.66±0.03
6e	SO ₂ Ph	268 [70±8]	6.58±0.07
6f	C(O)Ph	773 [85±6]	6.22±0.25
6g	C(O)2-pyridyl	564 [91±5]	6.25±0.03
6h	C(O)4-pyridyl	179 [85±7]	6.75±0.03

^aCalcium mobilization assays with hM₄/Gq15-CHO cells performed in the presence of an EC₂₀ fixed concentration of acetylcholine; values represent means from three (*n*=3) independent experiments performed in triplicate.

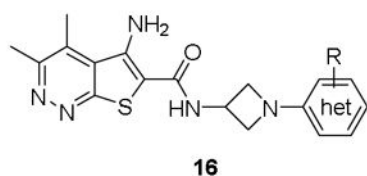
Table 2

Structures and activities for M₄ PAM analogs **16**.

 16			
Cmpd	R	hM ₄ EC ₅₀ (nM) ^a [% ACh Max ±SEM]	hM ₄ pEC ₅₀ (±SEM)
16a		439 [87±4]	6.36±0.04
16b		419 [89±6]	6.45±0.19
16c		106 [81±4]	7.04±0.16
16d		124 [81±9]	6.99±0.18
16e		34 [96±5]	7.48±0.09
16f		78 [80±11]	7.13±0.11
16g		41 [89±11]	7.41±0.11
16h		38 [83±10]	7.48±0.17



Cmpd	R	hM ₄ EC ₅₀ (nM) ^a [% ACh Max ±SEM]	hM ₄ pEC ₅₀ (±SEM)
16i		29 [82±5]	7.74±0.22
16j		76 [75±6]	7.12±0.08
16k		Inactive	Inactive
16l		17 [88±11]	7.77±0.01
16m		16 [90±7]	7.81±0.03
16n		185 [87±4]	6.80±0.19
16o		51 [86±6]	7.30±0.00

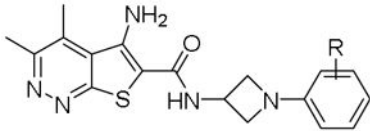
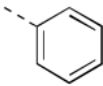
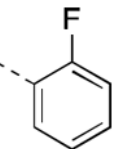
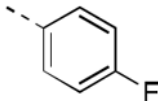
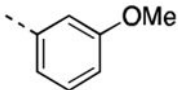
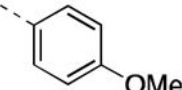
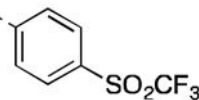
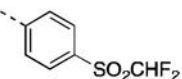
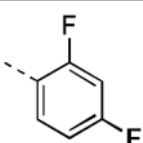


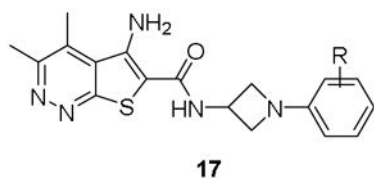
Cmpd	R	hM ₄ EC ₅₀ (nM) ^a [% ACh Max ±SEM]	hM ₄ pEC ₅₀ (±SEM)
16p		8 [86±3]	8.09±0.05
16q		11 [84±5]	7.97±0.09

^aCalcium mobilization assays with hM₄/Gq15-CHO cells performed in the presence of an EC₂₀ fixed concentration of acetylcholine; values represent means from three (*n*=3) independent experiments performed in triplicate.

Table 3

Structures and activities for M₄ PAM analogs **17**.

 17			
Cmpd	R	hM ₄ EC ₅₀ (nM) ^d [% ACh Max ±SEM]	hM ₄ pEC ₅₀ (±SEM)
17a		25 [85±8]	7.61±0.08
17b		28 [82±9]	7.56±0.03
17c		282 [77±8]	6.55±0.04
17d		141 [77±11]	6.88±0.11
17e		1289 [81±8]	5.90±0.06
17f		934 [86±1]	6.03±0.04
17g		325 [75±13]	6.63±0.29
17h		37 [94±9]	7.49±0.12



Cmpd	R	hM ₄ EC ₅₀ (nM) ^a [% ACh Max ±SEM]	hM ₄ pEC ₅₀ (±SEM)
17i		30 [84±5]	7.54±0.06
17j		19 [88±5]	7.73±0.06

^aCalcium mobilization assays with hM₄/Gqj5-CHO cells performed in the presence of an EC₂₀ fixed concentration of acetylcholine; values represent means from three (*n*=3) independent experiments performed in triplicate.